Digital Processing and Communication with Molecular Switches

By *Françisco M. Raymo**

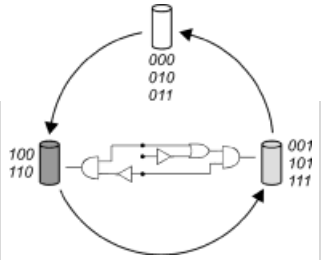

The tremendous pace in the development of information technology is rapidly approaching a limit. Alternative materials and operating principles for the elaboration and communication of data in electronic circuits and optical networks must be identified. Organic molecules are promising candidates for the realization of future digital processors. Their attractive features are the miniaturized dimensions and the high degree of control on molecular design possible in chemical synthesis. Indeed, nanostructures with engineered properties and specific functions can be assembled relying on the power of organic synthesis. In particular, certain molecules can be designed to switch from one state to another, when addressed with chemical, electrical, or optical stimulations, and to produce a detectable signal in response to these transformations. Binary data can be encoded on the input stimulations and output signals employing logic conventions and assumptions similar to those ruling digital electronics. Thus, binary inputs can be transduced into binary outputs relying on molecular switches. Following these design principles, the three basic logic operations (AND, NOT, and OR) and more complex logic functions (EOR, INH, NOR, XNOR, and XOR) have been reproduced already at the molecular level. Presently, these simple "molecular processors" are far from any practical application. However, these encouraging results demonstrate already that chemical systems can process binary data with designed logic protocols. Further fundamental studies on the various facets of this emerging area will reveal if and how molecular switches can become the basic components of future logic devices. After all, chemical computers are available already. We all carry one in our head!

1. Introduction

The miniaturization of electronic devices continues to deliver larger capacity memories and faster processors.[1] Increasing numbers of shrunk components are assembled on single chips to afford electronic circuits with growing integration densities. Transistors, for example, are scaled down at an exponential rate and their number on a chip doubles approximately every eighteen months.[1] The fabrication of small electronic devices becomes, however, more difficult and expensive as the nanometer scale is approached. The development of reliable techniques to produce conventional silicon-based devices with dimensions lower than 100 nm is a formidable technological challenge. Presumably, cost-effective miniaturization will not persist below this limit, which will be reached by the year 2005.[1] Furthermore, the bulk properties of semiconductors vanish at the nanometer level. Thus, the operating principles of present devices cannot survive the shrinking process.[2–4] These alarming limitations indicate that the tremendous pace of miniaturization will slow down and eventually stop soon.[5]

The increasing request for telecommunication and internet applications demands the continuous enhancement of the transmission capacity and speed of communication networks.[6] Present technology ensures the transport of hundreds of gigabits per second over hundreds of kilometers relying almost exclusively on optical connections.[7] Information is transferred in the form of optical signals propagating through interconnected optical fibers. Optoelectronic switches at the input and output ends of each fiber determine the routes of the traveling optical signals in response to electrical stimulations.[6,7] Unfortunately, the interplay between optical and electrical signals is a major "bottleneck" to the development of optical networks.[8,9] In principle, hundreds of optical signals with closely spaced wavelengths could be transmitted in parallel through a single waveguide. The propagating light beams would not interfere with each other. The non-interacting character of optical signals, however, does not apply to electrical signals. Only one electrical signal can be transported

[*] Prof. F. M. Raymo
Center for Supramolecular Science
Department of Chemistry
University of Miami
1301 Memorial Drive, Coral Gables, FL 33146-0431 (USA)
E-mail: fraymo@miami.edu

  0935-9648/02/0603-0401 $ 17.50+.50/0

through a single electrical wire. Thus, even although optical fibers can transmit multiple data in parallel, optoelectronic switches process them more or less sequentially. The only solution to this problem is to eliminate completely the electronic portion of these hybrid devices and to route the traveling optical signals with optical, rather than electrical, stimulations.[10–12]

The tremendous pace in the development of information technology demands the urgent identification of innovative designs for future data storage, elaboration, and communication devices. In particular, materials that would permit the manipulation of electrical and optical signals with alternative operating principles must be developed. Organic molecules are promising candidates for the realization of electronic and photonic devices.[13–16] They have nanoscaled dimensions. Their properties can be tuned through a wealth of chemical modifications. They are synthesized in massively parallel processes in which billions of them are produced simultaneously. They are relatively cheap to make even in large quantities.

Recently, the functions of memories, modulators, rectifiers, transistors, switches, and wires have been replicated using organic films or even single molecules.[17–24] Despite these remarkable examples, however, this research area is still at an exploratory stage. Reliable molecule-based electronic circuits and optical networks for practical applications are not a reality yet. Their design and fabrication remain more than a challenge.[22] Further fundamental studies on the various facets of this growing research field are needed. In particular, efficient and reliable mechanisms to elaborate signals with molecules must be identified and tested experimentally.

This review illustrates the fundamental principles of binary logic and highlights the chemical strategies that have been explored so far to implement digital processing and communication. Most of these methods rely on the simultaneous stimulation of large collections of molecules with chemical, electrical, and/or optical inputs. At this stage, they are far from the level of miniaturization required for the realization of nanoscaled processors. However, some of these strategies can be scaled down, at least in principle, to single molecules. It is important to note that the operating mechanisms of most of these chemical systems have little in common with those ruling conventional electronics. Acid/base reactions, conformational changes, photoinduced electron transfer, photoinduced isomerizations, redox processes, and supramolecular events dominate their behavior. With the exception of some molecule-based electronic devices, the principles controlling these chemical processors are much more similar to those governing information transfer in living organisms.

2. Logic Gates

In present computer networks, data are elaborated electronically by microprocessor systems and are exchanged optically between remote locations. Data processing and communication require the encoding of information in electrical and optical signals in the form of binary digits.[25] A threshold value and a logic convention are established for each signal. In a positive logic convention, a *0* is used to represent a signal that is below the threshold and a *1* is employed to indicate a signal that is above. For example, a threshold voltage of 2 V and a positive logic convention can be established for a certain electrical signal. A value of 5 V would be above the threshold and would correspond to a *1*. A value of 1 V would be below the threshold and would correspond to a *0*. In a negative logic convention, instead, the assignment is reversed. Using similar assumptions, the logic circuits of microprocessor systems elaborate binary data through sequences of logic gates. The symbols employed to represent the three basic logic gates and truth tables summarizing their operations are illustrated in Figure 1. These devices execute the three fundamental logic operations AND, NOT, and OR. The NOT operator converts the input signal ***I*** into the output signal ***O***. When ***I*** is *0*, ***O*** is 1. When ***I*** is *1*, ***O*** is *0*. Because of the inverse relationship between the input and output values, the NOT gate is often called inverter.[26] The OR operator combines the two input signals ***I*1** and ***I*2** into the output signal ***O***. When ***I*1** and/or ***I*2** is *1*, ***O*** is *1*. When ***I*1** and ***I*2** are *0*, ***O*** is *0*. The AND gate also combines two inputs into one output. In this instance, however, ***O*** is *1* only when both inputs are *1*. In the other three cases, ***O*** is *0*.

The output of one gate can be connected to one of the inputs of another operator. A NAND gate (Fig. 1), for example, is assembled connecting the output of an AND operator to

Françisco M. Raymo received a Laurea in Chemistry from the University of Messina (Italy) in 1992 and a Ph.D. in Chemistry from the University of Birmingham (UK) in 1996. He was a postdoctoral research fellow at the University of Birmingham (UK) from 1996–1997 and at the University of California, Los Angeles (USA) from 1997–1999. He was appointed Assistant Professor of Chemistry at the University of Miami in 2000. His research interests revolve around the design, synthesis, and analysis of functional materials incorporating molecular components. In particular, he is developing molecular switches for digital processing and communication and template-directed strategies to assemble surface coatings for chemical sensing. He is the author of more than 100 publications in the areas of computational chemistry, chemical synthesis, materials science, and supramolecular chemistry.

  0935-9648/02/0603-0402 $ 17.50+.50/0

ADVANCED MATERIALS

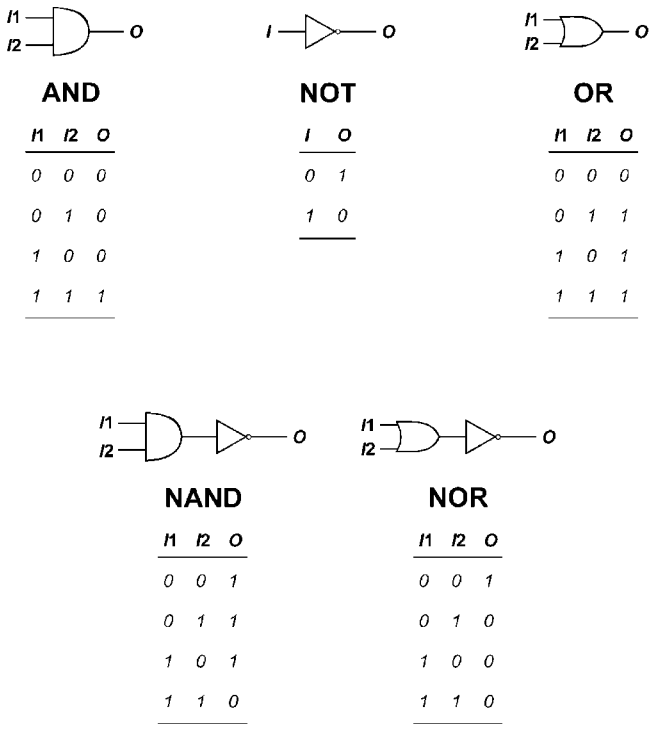

Fig. 1. The AND, NOT, and OR gates transduce one or two inputs (***I***) into a single output (***O***) through specific logic operations. The NAND and NOR gates are assembled connecting the output of AND and OR operators to the input of a NOT gate.

the input of a NOT gate. Now, the two inputs ***I*1** and ***I*2** are converted into the output ***O*** after two consecutive logic operations. Comparison of the truth tables of the AND and NAND gates reveals the inverse relationship between their output values imposed by the NOT operator incorporated in the NAND assembly. In a similar fashion, a NOR gate (Fig. 1) can be assembled connecting the output of an OR operator to the input of a NOT gate. Once again, two consecutive logic operations convert the two inputs ***I*1** and ***I*2** into the output ***O***. The NAND and NOR operations are termed universal functions because any conceivable logic operation can be implemented relying on one of these two gates only.[25] In fact, digital circuits are fabricated routinely interconnecting exclusively NAND or exclusively NOR operators.[26]

The logic gates of microprocessor systems are assembled interconnecting transistors and their input and output signals are electrical.[25] However, the concepts of binary logic could be extended to chemical, mechanical, optical, pneumatic, or any other type of signal. First, it is necessary to design devices that would respond to these signals in the same way transistors respond to electrical stimulations. The lack of an optical equivalent to a transistor has, in fact, limited considerably the development of optical computing.[27] In present communication networks, the binary data encoded into the propagating optical signals are actually routed electronically.[6,7] At the receiving end of each optical fiber, sophisticated optoelectronic devices convert the incident optical inputs into electrical signals. They process their binary content in this form before reconverting them into optical outputs, which finally escape through another optical fiber.

3. Molecular Switches

Certain organic molecules, called molecular switches,[28] adjust their structural and electronic properties when stimulated with chemical, electrical, or optical inputs. An example is illustrated schematically in Figure 2. A molecule switches from one state to another when stimulated with an input signal. The two states can be isomers, an acid and the conjugated base, the oxidized and reduced forms of a redox active molecule, or even the complexed and uncomplexed forms of a receptor.[28–37] Often, these transformations are reversible. The chemical system returns to the original state when the input signal is turned off. In some instances, the molecular switch produces a chemical, electrical, and/or optical output that varies in intensity with the switching process. For example, a change in pH, redox potential, absorbance, or emission intensity can accompany the interconversion between the two states of a molecular switch.[28–37]

The analogy between molecular switches and logic gates is obvious. They both convert input stimulations into output signals with intrinsic protocols. It follows that the principles of binary logic can be applied to the signal transduction operated by molecular switches. The analysis of their logic behavior requires, first of all, the assignment of threshold values and logic conventions to their input and output signals. The switching operation illustrated in Figure 2, for example, is based on the interplay between one input and one output. When the input is applied, the output changes from a low to a high value. We

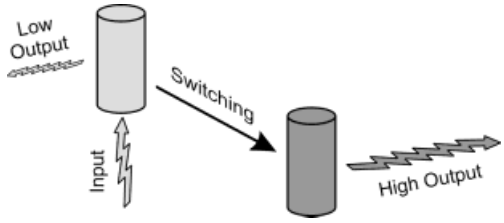

Fig. 2. The shaded cylinders represent two different states of a molecular switch. An input stimulation induces the transformation of one state into the other and determines the intensity of an output signal.

can assume arbitrary that the low value is below a fixed logic threshold and the high value is above. We can now apply either a positive or a negative logic convention. In a positive logic convention, a *0* corresponds to the low output and a *1* corresponds to the high output. In a negative logic convention, a *0* corresponds to the high output and a *1* corresponds to the low output. In the examples discussed in the following sections, we will extend a similar analysis to all signals applying, in most cases, positive logic conventions. It is interesting to note, however, that inputs and outputs do not need to share the same logic convention and that different conventions applied to the same device can lead to different logic func-

  0935-9648/02/0603-0403 $ 17.50+.50/0

tions.[25] Thus, in analogy to transistor–transistor logic (TTL) and complementary metal oxide semiconductor (CMOS) logic circuits,[26] the signal transduction protocol of a molecular switch can be programmed to execute specific logic functions simply by selecting the initial logic assumptions.

4. Molecular AND, NOT, and OR Gates

In most instances, molecular switches are addressed with chemical, electrical, or optical signals.[28–37] Alternative inputs, for example magnetic stimulations,[38] can be employed as well, but are less common. In response to these inputs, molecular switches produce outputs that, generally, are also chemical, electrical, or optical signals. Inputs and outputs, however, do not need to belong to the same category. For example, photochromic switches convert optical inputs into optical outputs, but electrochromic switches transduce electrical inputs into optical outputs.[28–37] The result of a logic operation is, in fact, controlled solely by the values of the binary digits encoded on the inputs and outputs.[25] The nature of these signals is irrelevant.

A NOT gate has only one input and one output. At the molecular level, this simple logic function can be reproduced using one of the nine input/output combinations illustrated in Figure 3. A closer inspection of this diagram reveals that some of the input/output transduction mechanisms listed correspond to established phenomena in the chemical sciences. Fluorescence quenching (C), electrochromism (F), photoinduced proton transfer (G), photovoltage generation (H), and photochromism (I) are only some of the many phenomena

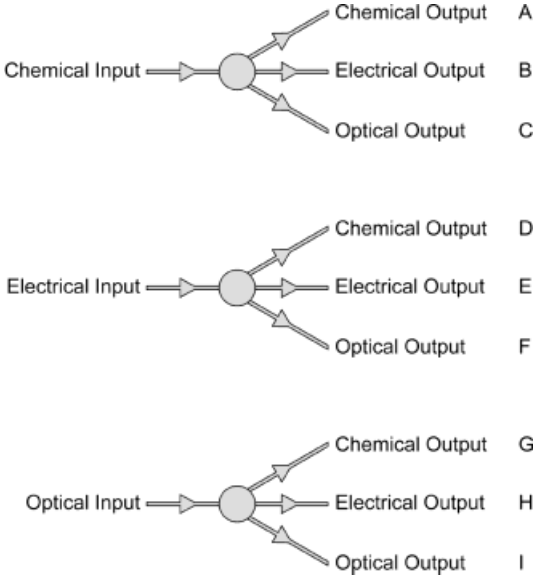

Fig. 3. Nine signal transduction mechanisms (A–I) can be envisaged at the molecular level to execute logic operations that require only one input and one output. This analysis is limited to molecular switches that respond to chemical, electrical, or optical inputs producing chemical, electrical, or optical outputs. Of course, alternative signals (e.g., magnetic stimulations) can enter this diagram and increase the number of mechanisms potentially available to implement logic operations with chemical systems.

that can enter this diagram. Thus, hundreds, if not thousands, of chemical systems that can execute NOT operations are known already. Of course, the logic behavior of most of them has not been analyzed or even recognized.

More than a decade ago, Aviram proposed a potential strategy to execute logic operations at the molecular level.[39] Later, de Silva recognized the analogy between molecular switches and logic gates in a seminal article.[40] He reproduced AND, NOT, and OR operations with fluorescent molecules. The pyrazoline derivative **1** (Fig. 4) is one of them. It executes NOT operations transducing a chemical input into an optical output (C in Figure 3). The fluorescence quantum yield of **1** is 0.13 in the presence of only 10^{-1} equivalents of HCl in a mixture of CH_3OH and H_2O (1:4, v/v).[41] The quantum yield drops to 0.003 when the equivalents of H^+ are 10^3. Photoinduced electron transfer from the central pyrazoline unit to the pendant benzoic acid quenches the fluorescence of the protonated form. Thus, a change in H^+ concentration (***I***) from a low to a high value switches the emission intensity (***O***) from a high to a low value. The inverse relationship between the chemical input ***I*** and the optical output ***O*** translates into the truth table of a NOT operation (Fig. 1) if a positive logic convention (low = *0*, high = *1*) is applied to both signals. The emission intensity is high (***O*** = *1*) when the concentration of H^+ is low (***I*** = *0*) and vice versa.

A NOT operator has one input and one output. It is, therefore, a two-terminal gate. Instead, AND and OR operators have two inputs and one output. They are three-terminal gates. The addition of one input terminal raises the number of signal transduction mechanisms from 9 (Fig. 3) to 27. In principle, all 27 inputs/output combinations can be used to implement AND and OR operations at the molecular level. However, most of the molecular AND and OR gates developed so far have two chemical inputs and one optical output.[40,42–49] Examples of molecular switches able to process chemical and optical inputs into optical outputs with AND functions are also known.[50–53] A notable exception is an ultrafast molecular AND gate that transduces two optical inputs into an optical output.[54] Alternative signal transduction schemes have also been proposed.[55,56]

Two representative examples of molecular three-terminal gates are illustrated in Figure 4. The anthracene derivatives **2** and **3** respond to two chemical inputs producing an optical output. The signal transduction mechanism of the criptand **2** corresponds to an OR operation,[47] while that of the crown ether **3** is equivalent to an AND function.[48] In THF, the fluorescence quantum yield of the criptand **2** is only 0.001 in the absence of transition metal cations. Photoinduced electron transfer from the tertiary nitrogen atoms to the appended anthracene units quenches the fluorescence. In the presence of 10^3 equivalents of Cu^{II} and/or Ni^{II}, the quantum yield increases by approximately two orders of magnitude. In fact, the complexation of a transition metal cation inside the criptand depresses the efficiency of photoinduced electron transfer. It is worth noting that the two chemical inputs of this[47] and other[40,42,44] molecular OR gates cannot address simulta-

  0935-9648/02/0603-0404 $ 17.50+.50/0

ADVANCED MATERIALS

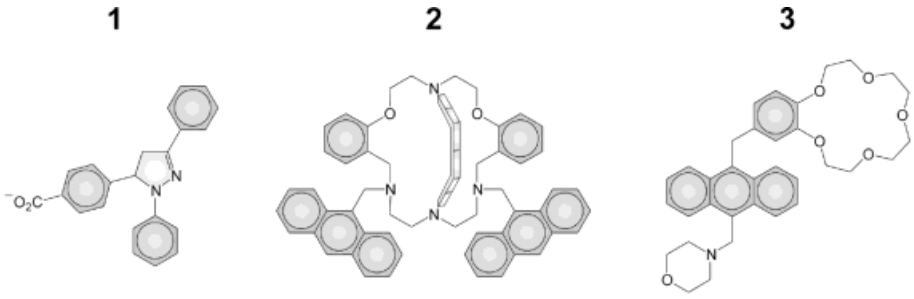

H^+	Emission
Low	High
High	Low

Cu^{II}	Ni^{II}	Emission
Low	Low	Low
Low	High	High
High	Low	High
High	High	High

H^+	Na^+	Emission
Low	Low	Low
Low	High	Low
High	Low	Low
High	High	High

Fig. 4. The fluorescence intensity of the pyrazoline derivative **1** is high when the concentration of H^+ is low and vice versa. The fluorescence intensity of the criptand **2** is high when the concentration of Cu^{II} and/or Ni^{II} is high. The emission is low when both concentrations are low. The fluorescence intensity of the crown ether **3** is high only when the concentrations of H^+ and Na^+ are high. The emission is low in the other three cases. The signal transductions of the molecular switches **1**, **2**, and **3** translate into the truth tables of NOT, OR, and AND gates, respectively, if a positive logic convention is applied to all inputs and outputs (low = *0*, high = *1*). Note that one of the three identical fragments linking the bridgehead nitrogen atoms of the criptand **2** is omitted for clarity. A cartoon representation is shown instead.

neously a single molecule. The two transition metals cannot be accommodated inside the very same criptand. Nonetheless, these systems have been interpreted as three-terminal gates in the original articles,[40,42,44,47] considering the two chemical inputs to be independent.

A similar effect is observed for the anthracene derivative **3**. In MeOH, the fluorescence quantum yield of the deprotonated form of **3** is only 0.0024 in the absence of metal cations. Photoinduced electron transfer from either the tertiary nitrogen atom or the dioxybenzene ring to the anthracene unit quenches the fluorescence. A significant enhancement in quantum yield is observed only when the efficiencies of both photoinduced electron transfer processes are depressed. The concomitant addition of 10^3 equivalents of H^+ and 10^4 equivalents of Na^+ results in the protonation of the tertiary nitrogen atom and in the inclusion of the metal cation in the crown ether cavity. Under these conditions, the quantum yield raises to 0.22. Instead, it remains below 0.01 when only one of the two chemical inputs (H^+ or Na^+) is applied.

The molecular switches **2** and **3** respond to two chemical inputs (***I*1** and ***I*2**) producing one optical output (***O***). The two inputs ***I*1** and ***I*2** and the single output ***O*** switch between low and high values. If a positive logic convention (low = *0*, high = *1*) is applied to all signals, the signal transduction behavior of **2** translates into the truth table of an OR operator (Fig. 1) and that of **3** corresponds to the truth table of an AND gate. In fact, only one chemical input (***I*1** or ***I*2** = *1*) is sufficient to enhance the optical output (***O*** = *1*) of **2**, but both inputs (***I*1** and ***I*2** = *1*) are needed to stimulate the optical output (***O*** = *1*) of **3**. The comparison of these two chemical systems shows that similar operating principles can be exploited to process different logic functions with fluorescent molecules.

5. Combinational Logic Circuits

Combinational logic circuits are assembled connecting AND, NOT, and OR gates.[25] The NAND and NOR operators (Fig. 1) and the enabled OR (EOR), exclusive NOR (XNOR), exclusive OR (XOR), two- and three-input inhibit (INH) operators (Fig. 5) are simple examples of combinational logic circuits. Their logic functions can be reproduced at the molecular level with only one molecular switch. In fact, the interplay of chemical and/or optical inputs and optical outputs has been exploited already to execute two-input INH,[57] and three-input INH,[58] EOR,[59] NOR,[58] and XOR[60,61] operations. One representative example is illustrated in Figure 6. The Tb^{III} complex **4** transduces two chemical inputs into one optical output through an INH operation. In either aerated or degassed alkaline solution (pH 11), the complex has a weak emission band at 548 nm (λ_{exc} = 330 nm).[57] A 50-fold increase in the emission intensity is observed in acidic conditions (pH 2.9) only if O_2 is absent. The protonation of the quinoline nitrogen atom influences the mechanism of energy transfer from the quinoline excited state to the lanthanide excited state enhancing the emission intensity. The O_2, however, depresses the efficiency of energy transfer quenching the quinoline triplet state T_1 that is involved in this process. Thus, the emission intensity (***O***) is high only when the concentration of H^+ (***I*1**) is high and that of O_2 (***I*2**) is low. If a positive logic convention (low = *0*, high = *1*) is applied to all signals, the signal transduction behavior of **4** translates into the truth table of a two-input INH circuit (Fig. 5). The output ***O*** is equal to *1* only when ***I*1** is *1* and ***I*2** is *0*.

The implementation of combinational logic circuits at the molecular level is certainly not limited to the use of chemical inputs. Electrical signals, for example, can control the output of a molecular switch stimulating reversible redox processes. A XNOR operation can be executed relying on this operating principle. In the supramolecular assembly **5** (Fig. 6), a π-electron rich tetrathiafulvalene (TTF) derivative is inserted through the cavity of a π-electron deficient bipyridinium (BIPY) cyclophane. In MeCN, an absorption band associated with the charge-transfer interactions between the complementary π-surfaces is observed at 830 nm.[62] Electrical stimulations alter the redox state of either the TTF or the BIPY units encouraging the separation of the two components of the complex and the disappearance of the charge-transfer band.

  0935-9648/02/0603-0405 $ 17.50+.50/0

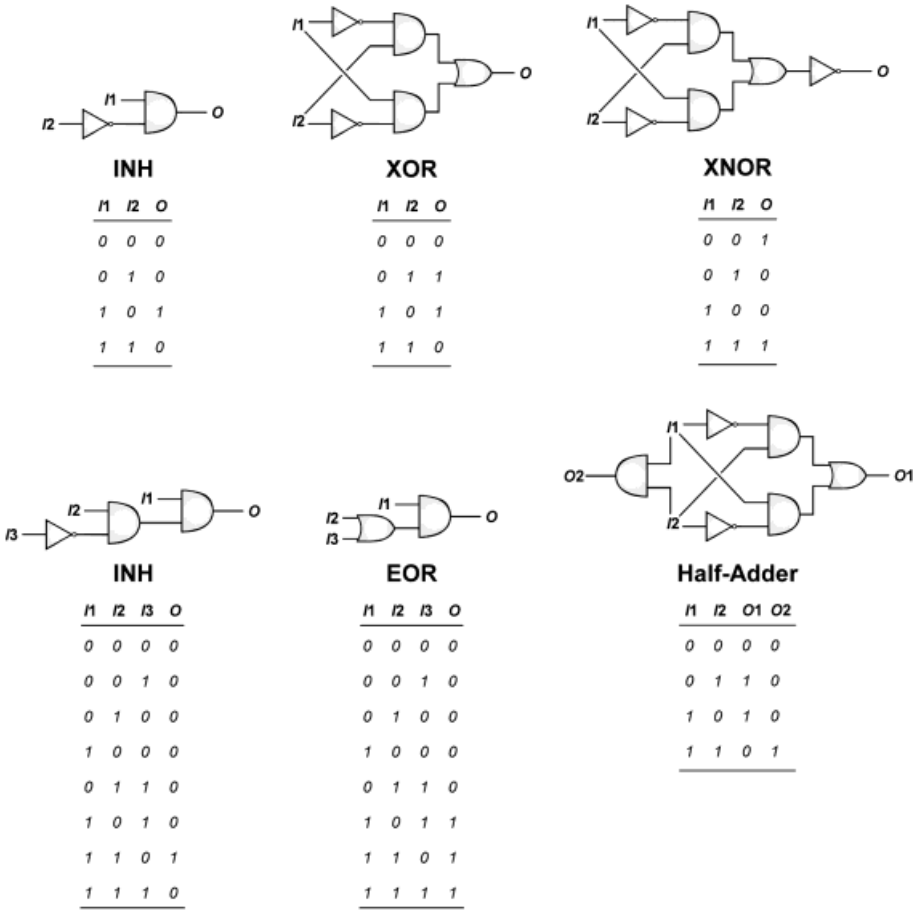

Fig. 5. The two-input INH, XNOR, and XOR circuits transduce two inputs (***I*1** and ***I*2**) into a single output (***O***). The EOR and the three-input INH convert three inputs (***I*1**, ***I*2**, and ***I*3**) into one output (***O***). The half-adder circuit transduces two inputs (***I*1** and ***I*2**) into two outputs (***O*1** and ***O*2**).

In particular, electrolysis at a potential of +0.5 V oxidizes the neutral TTF unit to a monocationic form, which is expelled from the tetracationic cavity of the cyclophane. Consistently, the absorption band at 830 nm disappears. The charge-transfer band, however, is restored fully after the exhaustive back reduction of the TTF unit at a potential of 0 V. Similar changes in the absorption properties can be induced addressing the BIPY units. Electrolysis at –0.3 V reduces the dicationic BIPY units to their monocationic forms encouraging the separation of the two components of the complex and the disappearance of the absorption band. The original absorption spectrum is restored after the exhaustive back oxidation of the BIPY units at a potential of 0 V. In summary, electrical stimulations control the charge-transfer absorbance (***O***). The signal transduction of this chemical system was analyzed considering two independent redox inputs in the original article.[62] One of them (***I*1**) controls the redox state of the TTF unit switching between 0 and +0.5 V. The other (***I*2**) determines the redox state of the bipyridinium units switching between –0.3 and 0 V. A positive logic convention (low = *0*, high = *1*) was applied to the input ***I*1** and output ***O***. A negative logic convention (low = *1*, high = *0*) was applied to the input ***I*2**. The resulting truth table corresponds to that of a XNOR circuit (Fig. 5). The charge-transfer absorbance is high (***O*** = *1*) only when one voltage input is low and the other is high (***I*1** = *0*, ***I*2** = *0*) or vice versa (***I*1** = *1*, ***I*2** = *1*). It is important to note that the input string with both ***I*1** and ***I*2** equal to *1* implies that input potentials of +0.5 and –0.3 V are applied simultaneously to a solution containing the supramolecular assembly **5** and not to an individual complex. Of course, the concomitant oxidation of the TTF guest and reduction of the BIPY units in the very same complex would be unrealistic. In bulk solution, instead, some complexes are oxidized while others are reduced, leaving the average solution composition unaffected. Thus, the XNOR operation executed by this supramolecular systems is a consequence of bulk properties and not a result of unimolecular signal transduction.

The EOR, INH, NOR, XNOR, and XOR operations are relatively simple and one molecular switch is sufficient to execute these logic functions.[57–62] The half-adder (Fig. 5), instead, requires two molecular switches. This particular combinational logic circuit processes the addition of two input digits (***I*1** and ***I*2**) operating an AND gate and a XOR circuit in parallel. The XOR portion of the half-adder converts the two inputs ***I*1** and ***I*2** into the output ***O*1**. The AND gate converts the same two inputs into the other output ***O*2**. The role of the two outputs ***O*1** and ***O*2** in binary additions is equivalent to that of the unit and ten digits in decimal arithmetic. Decimal digits range from 0 to 9. The result of the addition of two decimal digits can range from 0 to 18. The first ten values (0–9) can be represented with one decimal digit. The other nine values (10–18) must be represented with two digits. For example, the number 13 is written using a unit digit (3) and a ten digit (1). Similarly, binary digits range from *0* to *1*. The result of the addition of two binary digits can be *0*, *1*, or *10*. The first two values (*0* and *1*) can be represented with one binary digit. The third value (*10*) requires two binary digits in analogy to decimal numbers greater than 9. Thus, the half-adder must have two binary outputs (***O*1** and ***O*2**) to represent the three possible results of the addition of the two binary inputs (***I*1** and ***I*2**).

The logic function of the half-adder can be implemented using two molecular switches. One of them executes the XOR operation and affords ***O*1**. The other executes the AND op-

0935-9648/02/0603-0406 $ 17.50+.50/0

ADVANCED MATERIALS

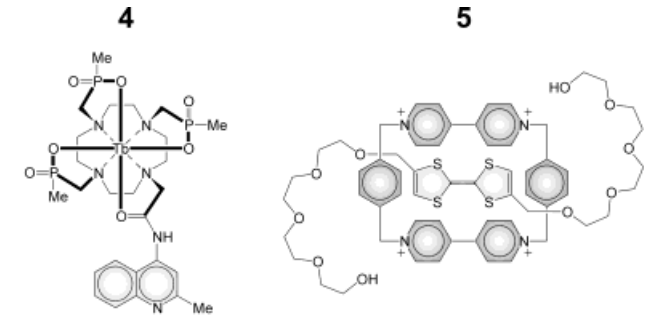

H^+	O_2	Emission
Low	Low	Low
Low	High	Low
High	Low	High
High	High	Low

TTF	BIPY	Absorbance
Low	Low	High
Low	High	Low
High	Low	Low
High	High	High

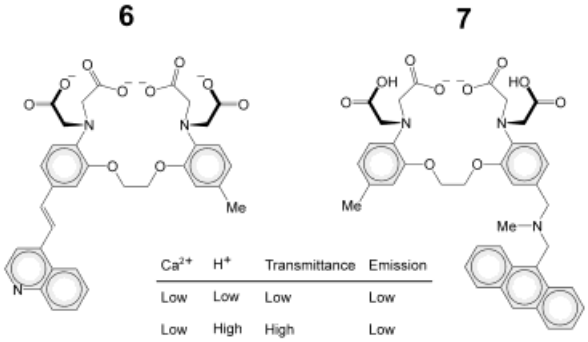

Ca^{2+}	H^+	Transmittance	Emission
Low	Low	Low	Low
Low	High	High	Low
High	Low	High	Low
High	High	Low	High

Fig. 6. The emission intensity of the Tb^{III} complex **4** is high when the concentration of H^+ is high and the concentration of O_2 is low. The signal transduction of **4** translates into the truth tables of the two-input INH if a positive logic convention is applied to all inputs and outputs (low = *0*, high = *1*). The charge-transfer absorbance of the complex **5** is high when the voltage input addressing the tetrathiafulvalene (TTF) unit is low and that stimulating the bipyridinium (BIPY) units is high and vice versa. If a positive logic convention is applied to the TTF input and to the absorbance output (low = *0*, high = *1*) while a negative logic convention is applied to the BIPY input (low = *0*, high = *1*), the signal transduction of **5** translates into the truth table of a XNOR circuit. The transmittance of the quinoline derivative **6** is high when the concentration of Ca^{2+} is low and the concentration of H^+ is high and vice versa. The fluorescence intensity of the anthracene derivative **7** is high only when the concentration of Ca^{2+} is high and the concentration of H^+ is high. The two molecular switches **6** and **7** share the same two inputs and, when operated in parallel, they reproduce the logic function of the half-adder if a positive logic convention (low = *0*, high = *1*) is applied to all inputs and outputs.

eration and affords ***O2***. The two independent molecular switches, however, must respond to the same two inputs ***I1*** and ***I2***. The tetracarboxylate receptors **6** and **7** (Fig. 6) satisfy these conditions. In H_2O, the quinoline derivative **6** has an absorption band at 390 nm with a transmittance of 5 %.[63] Upon addition of ca. 10^3 equivalents of Ca^{2+}, the transmittance increases to 49 %. This enhancement is a result of a hypsochromic shift of the absorption band caused by the complexation of the metal cation in the tetracarboxylate cleft. Similarly, the addition of 10 equivalents of H^+ raises the transmittance to 39 % as a result of a bathochromic shift induced by the protonation of the quinoline nitrogen atom. Instead, the transmittance remains low when the two chemical inputs are applied simultaneously. Thus, the transmittance at 390 nm (***O1***) is high when the concentration of Ca^{2+} (***I1***) is high and that of H^+ (***I2***) is low and vice versa. Under the same experimental conditions, the fluorescence quantum yield of the anthracene derivative **7** is only 0.006. Photoinduced electron transfer from either the tetracarboxylate receptor or the tertiary nitrogen atom appended to the anthracene unit quenches the emission. The efficiencies of both processes are depressed when Ca^{2+} and H^+ are added simultaneously. Only then, the quantum yield raises to 0.21. Thus, the fluorescence intensity (***O2***) is high only when the concentrations of Ca^{2+} (***I1***) and H^+ (***I2***) are both high. When the two molecular switches **6** and **7** are codissolved in H_2O, they can be operated in parallel with the two inputs ***I1*** and ***I2***. Of course, individual molecular switches cannot share the very same Ca^{2+} and H^+ ions. They actually share the same type of chemical inputs producing in response the two outputs ***O1*** and ***O2***. If a positive logic convention (low = *0*, high = *1*) is applied to all signals, the signal transduction behavior of the two molecular switches translates into the truth table of the half-adder (Fig. 5).

The EOR and the three-input INH (Fig. 5) transduce three inputs into a single output.[58,59] Alternative transduction protocols to convert three inputs into one or two outputs at the molecular level are possible.[64] In particular, we have developed a three-state molecular switch (Fig. 7) that responds to two optical inputs (***I1*** and ***I2***) and one chemical input (***I3***) producing two optical outputs (***O1*** and ***O2***).[65] Binary digits can be encoded on each signal applying positive logic conventions (low = *0*, high = *1*). It follows that the three-state molecular switch converts input strings of three binary digits into output strings of two binary digits. The corresponding truth table and equivalent logic circuit are illustrated in Figure 7. One portion of this complex logic circuit converts the three inputs ***I1***, ***I2***, and ***I3*** into the output ***O1*** through AND, NOT, and OR operations. The other fragment transduces the same inputs into the output ***O2*** through AND and NOT operations.

The three-state molecular switch is operated in MeCN. The three input stimulations are ultraviolet light (***I1***), visible light (***I2***), and H^+ (***I3***). One of the two optical outputs is the absorbance at 401 nm (***O1***), which is high when the molecular switch is in the yellow-green state **MEH** and low in the other two cases. The other optical output is the absorbance at 563 nm (***O2***), which is high when the molecular switch is in the purple state **ME** and low in the other two cases. The colorless spiropyran state **SP** switches to the merocyanine form **ME** upon irradiation with ultraviolet light. It switches to the protonated merocyanine from **MEH** when treated with H^+. The colored state **ME** isomerizes back to **SP** upon irradiation with visible light. Alternatively, **ME** switches to **MEH** when treated with H^+. The colored state **MEH** switches to **SP**, when irradiated with visible light, and to **ME**, after the removal of H^+. Thus, the optical output ***O1*** is high (***O1*** = *1*) when only the input ***I3*** is applied (***I1*** = *0*, ***I2*** = *0*, ***I3*** = *1*), when only the

  0935-9648/02/0603-0407 $ 17.50+.50/0

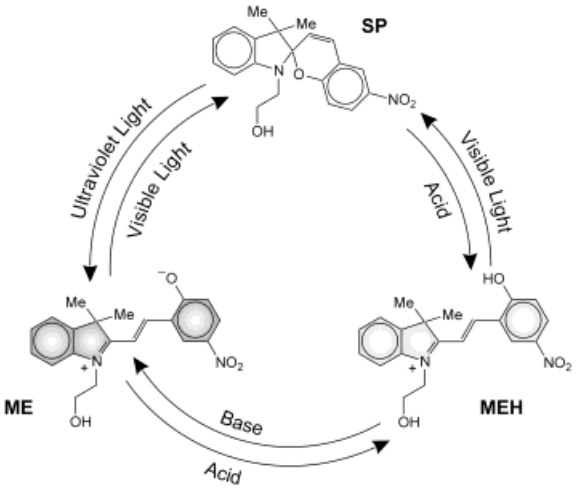

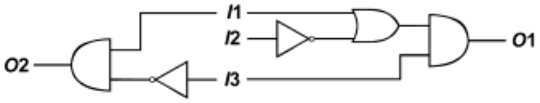

I1	I2	I3	O1	O2
0	0	0	0	0
0	0	1	1	0
0	1	0	0	0
1	0	0	0	1
0	1	1	0	0
1	0	1	1	0
1	1	0	0	1
1	1	1	1	0

Fig. 7. Ultraviolet light (***I1***), visible light (***I2***), and H^+ (***I3***) inputs induce the interconversion between the three states **SP**, **ME**, and **MEH**. The colorless state **SP** does not absorb in the visible region. The yellow–green state **MEH** absorbs at 401 nm (***O1***). The purple state **ME** absorbs at 563 nm (***O2***). The truth table illustrates the conversion of input strings of three binary digits (***I1***, ***I2***, and ***I3***) into output strings of two binary digits (***O1*** and ***O2***) operated by this three-state molecular switch. A combinational logic circuit incorporating nine AND, NOT, and OR operators correspond to this particular truth table.

input ***I2*** is not applied (***I1*** = *1*, ***I2*** = *0*, ***I3*** = *1*), or when all three inputs are applied (***I1*** = *1*, ***I2*** = *1*, ***I3*** = *1*). The optical output ***O2*** is high (***O2*** = *1*) when only the input ***I1*** is applied (***I1*** = *1*, ***I2*** = *0*, ***I3*** = *0*) or when only the input ***I3*** is not applied (***I1*** = *1*, ***I2*** = *1*, ***I3*** = *0*). The combinational logic circuit shows that all three inputs determine the output ***O1***, while only ***I1*** and ***I3*** control the value of ***O2***.

6. Digital Communication

A NAND operator (Fig. 1) is assembled connecting the output terminal of an AND gate to the input terminal of a NOT gate.[25] In the resulting circuit, the first gate receives the two inputs ***I1*** and ***I2*** and converts them into a single signal according to an AND operation. This signal is then transmitted to the second gate and transduced into the final output ***O*** after a NOT operation. The physical connection between the two gates is responsible for their communication and is, of course, essential for the execution of the NAND function. Similarly, the combinational logic circuits illustrated in Figure 5 are assembled connecting the output and input terminals of several AND, NOT, and OR gates. The digital communication between these basic logic elements ensures the execution of a sequence of simple logic operations that results in the complex logic function processed by the entire circuit. Obviously, the logic function of a given circuit can be adjusted altering the number and type of basic gates and their interconnection protocol. This modular approach to combinational logic circuits is extremely powerful. Any logic function can be implemented connecting the appropriate combination of simple AND, NOT, and OR gates.

The strategy followed so far to implement complex logic functions with molecular switches is based on the careful design of the chemical system and on the judicious choice of the inputs and outputs.[57–62] A specific sequence of AND, NOT, and OR operations is "programmed" in a single molecular switch. No digital communication between distinct gates is needed since they are "built in" the same molecular entity. Though extremely elegant, this strategy does not have the same versatility of a modular approach. A different molecule has to be designed, synthesized, and analyzed every single time a different logic function has to be realized. In addition, the degree of complexity that can be achieved with only one molecular switch is fairly limited. The "connection" of the input and output terminals of independent molecular AND, NOT, and OR operators, instead, would offer the possibility of assembling any combinational logic circuit from three basic building blocks. The closest example to a modular approach at the molecular level is the operation of the molecular AND and XOR gates **6** and **7** to execute the half-adder function.[63] In this case, however, the two molecular switches are operated in parallel and there is no need of digital communication between them.

In digital electronics, the communication between two logic gates can be realized by connecting their terminals with a wire.[26] Methods to transmit binary data between distinct molecular switches are not so obvious and must be identified. Recently, we have developed two strategies to communicate signals between compatible molecular components.[66–68] Both methods rely on the three-state molecular switch illustrated in Figure 7. In one instance, a chemical signal is communicated between two distinct molecular switches.[67] In fact, the state **ME** is a photogenerated base. The basic phenolate group produced upon irradiation of the colorless state **SP** with ultraviolet light can abstract a proton from an acid present in the same solution. The state **MEH** is, instead, a photoacid. It releases H^+ upon irradiation with visible light and can protonate a base codissolved in the same medium. Thus, photoinduced proton transfer can be exploited to communicate a chemical signal from the three-state molecular switch to another H^+

  0935-9648/02/0603-0408 $ 17.50+.50/0

ADVANCED MATERIALS

sensitive molecular switch. For example, the orange azopyridine derivative **AZ** (Fig. 8) switches to the red–purple azopyridinium state **AZH** upon protonation.[67] This process is reversible and the addition of a base restores the orange state **AZ**. The two colored forms have different absorption properties in the visible region. In MeCN, the orange state **AZ** absorbs at 422 nm and the red–purple state **AZH** absorbs at 556 nm. The changes in absorbance of these two bands can be exploited to monitor the switching process. This two-state molecular switch transduces a chemical input (concentration of H^+) into one optical output (absorbance change at 422 or 556 nm). When the three-state molecular switch and the two-state molecular switch are codissolved in MeCN, they can be operated sequentially. In the presence of one equivalent of H^+, the two-state molecular switch is in state **AZH** and the absorbance at 556 nm is high (***O*** = *1*). Upon irradiation with ultraviolet light (***I*1** = *1*), **SP** switches to **ME**. The photogenerated base deprotonates **AZH** producing **AZ** and **MEH**. As a result, the absorbance at 556 nm decreases (***O*** = *0*). Upon irradiation with visible light (***I*2** = *1*), **MEH** switches to **SP** releasing H^+. The result is the protonation of **AZ** to form **AZH** and restore the high absorbance at 556 nm (***O*** = *1*). In summary, the three-state molecular switch transduces two optical inputs (***I*1** = ultraviolet light, ***I*2** = visible light) into a chemical signal (proton transfer) that is communicated to the two-state molecular switch and converted into a final optical output (***O*** = absorbance at 556 nm).

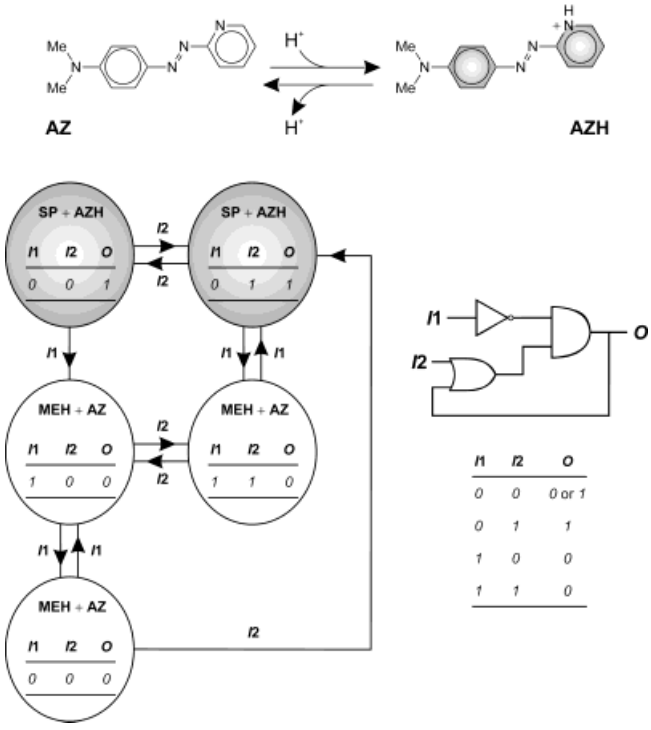

I1	I2	O
0	0	0 or 1
0	1	1
1	0	0
1	1	0

Fig. 8. The concentration of H^+ controls the reversible interconversion between the two states **AZ** and **AZH**. In response to ultraviolet light (***I*1**) and visible light (***I*2**) inputs, the three-state molecular switch in Figure 7 modulates the ratio between these two forms and the absorbance (***O***) of **AZH** through photoinduced proton transfer. The truth table and sequential logic circuit illustrate the signal transduction behavior of the two communicating molecular switches. The interconversion between the five three-digit strings of input (***I*1** and ***I*2**) and output (***O***) data is achieved varying the input values in steps.

The logic behavior of the two communicating molecular switches is significantly different from those of the chemical systems listed in Figures 4 and 6.[67] The truth table in Figure 8 lists the four possible combinations of two-digit input strings and the corresponding one-digit output. The output digit ***O*** for the input strings *01*, *10*, and *11* can take only one value. In fact, the input string *01* is transduced into a *1* and the input strings *10* and *11* are converted into *0*. The output digit ***O*** for the input string *00*, instead, can be either *0* or *1*. The sequence of events leading to the input string *00* determines the value of the output. The diagram in Figure 8 illustrates this effect. The five ovals represent the five three-digit input/output strings. The transformation of one oval into any of the other four is achieved in one or two steps changing the values of ***I*1** and/or ***I*2**. In two instances (shaded ovals), the two-state molecular switch is in state **AZH** and the output signal is high (***O*** = *1*). In the other three cases (non-shaded ovals), the two-state molecular switch is in state **AZ** and the output signal is low (***O*** = *0*). The strings *000* (bottom left) and *001* (top left) correspond to the first entry of the truth table. They share the same input digits, but differ in the output value. The string *000* (bottom left) can be obtained only from the string *100* (center left) varying the value of ***I*1**. Similarly, the string *001* (top left) can be accessed only from the string *011* (top right) varying the value of ***I*2**. In both transformations, the output digit remains unchanged. Thus, the value of ***O*1** in the parent string is memorized and maintained in the daughter string when both inputs become *0*. This memory effect is the fundamental operating principle of sequential logic circuits,[25] which are used extensively to assemble the memory elements of modern microprocessors. The sequential logic circuit equivalent to the truth table of the two communicating molecular switches is also illustrated in Figure 8. In this circuit, the input data ***I*1** and ***I*2** are combined through NOT, OR, and AND operators. The output of the AND gate ***O*** is also an input of the OR gate and controls, together with ***I*1** and ***I*2**, the signal transduction behavior.

The other strategy that we have developed for digital transmission between molecules is based on the communication of optical signals between the three-state molecular switch (Fig. 7) and fluorescent compounds.[66,68] We have assembled an optical network (Fig. 9) in which three optical signals (light-shaded arrows) travel from an excitation source to a detector after passing through two quartz cells.[68] Cell A contains an equimolar MeCN solution of naphthalene, anthracene, and tetracene. Cell B contains a MeCN solution of the three-state molecular switch. The excitation source sends three consecutive monochromatic light beams to cell A, stimulating the emission of the three fluorophores. The light emitted in the direction perpendicular to the exciting beam reaches cell B. When the molecular switch is in state **SP**, the naphthalene emission at 335 nm is absorbed and a low intensity output (***O*1**) reaches the detector. Instead, the anthracene

  0935-9648/02/0603-0409 $ 17.50+.50/0

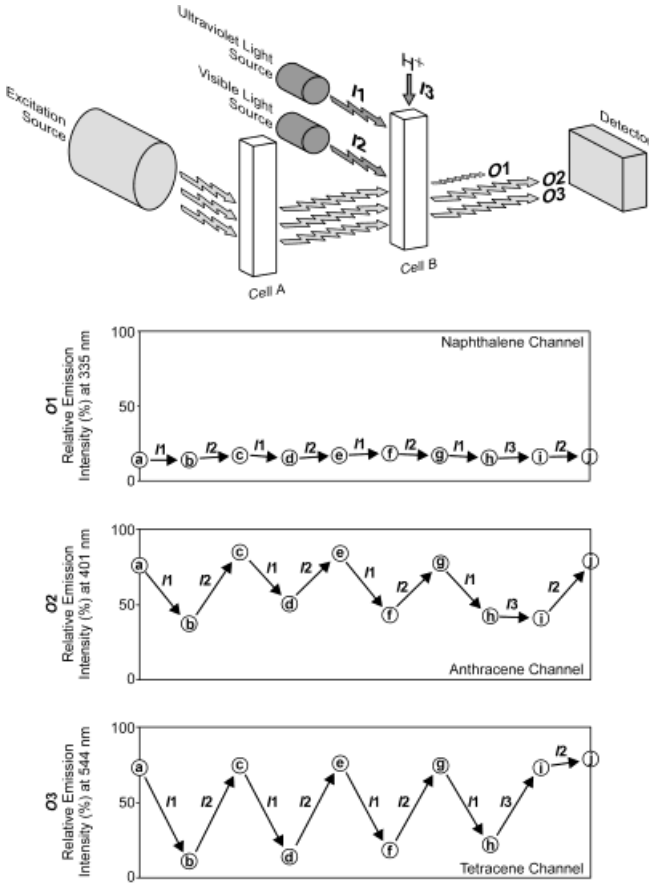

Fig. 9. The excitation source sends three monochromatic light beams (275, 357, and 441 nm) to cell A, which contains an equimolar MeCN solution of naphthalene, anthracene, and tetracene. The three fluorophores absorb the exciting beams and reemit at 305, 401, and 544 nm, respectively. The light emitted in the direction perpendicular to the exciting beams passes through cell B, which contains a MeCN solution of the three-state molecular switch shown in Figure 7. Ultraviolet light (***I*1**), visible light (***I*2**), and H^+ (***I*3**) inputs control the interconversion between the three states of the molecular switch and determine the intensity of the optical outputs (***O*1**, ***O*2**, and ***O*3**) reaching the detector. The naphthalene emission is absorbed equally by the three states of he molecular switch and the intensity of the output ***O*1** is always low (***a*–*j*** in the top plot). The anthracene emission is absorbed by two of the three states of the molecular switch and the intensity of the output ***O*2** oscillates between two values (***a*–*j*** in the center plot). A similar effect is observed for the intensity of the output ***O*3** (***a*–*j*** in the bottom plot), since the tetracene emission is absorbed by only one of the three states of the molecular switch. The state **MEH** of the molecular switch, however, has a different influence on the intensities of the outputs ***O*2** and ***O*3**. This state absorbs the emission of anthracene but not that of tetracene. As a result, the intensity of ***O*2** is low and that of ***O*3** is high (***i*** in the center and bottom plots).

and tetracene emissions at 401 and 544 nm, respectively, pass unaffected and high-intensity outputs (***O*2** and ***O*3**) reach the detector. When the molecular switch is in the **MEH** state, the naphthalene and anthracene emissions are absorbed and only the tetracene emission reaches the detector (***O*1** = *0*, ***O*2** = *0*, ***O*3** = *1*). When the molecular switch is in the **ME** state, the emission of all three fluorophores is absorbed (***O*1** = *0*, ***O*2** = *0*, ***O*3** = *0*). The interconversion of the molecular switch between the three states is induced addressing cell B with ultraviolet light (***I*1**), visible light (***I*2**), and H^+ (***I*3**) inputs (dark-shaded arrows). Thus, three independent optical outputs (***O*1**, ***O*2**, and ***O*3**) can be modulated stimulating the molecular switch with two optical and one chemical input. The three plots in Figure 9 illustrate this effect. The intensity of the naphthalene channel (***O*1**) is always low. The three states of the molecular switch absorb equally the light emitted by this fluorophore before detection. The intensities of the anthracene and tetracene channels (***O*2** and ***O*3**) switch between high and low values as the molecular switch changes between the states **SP** and **ME**. In fact, **SP** does not absorb these signals but **ME** does. In the case of the anthracene channel (***O*2**), the interconversion between **ME** and **MEH** maintains the output intensity low, since this state also absorbs the anthracene emission. In the case of the tetracene channel (***O*3**), switching between **ME** and **MEH** raises the output intensity, since **MEH** does not absorb at 544 nm. The truth table in Figure 10 illustrates the relation between the three inputs (***I*1**, ***I*2**, and ***I*3**) and the three outputs

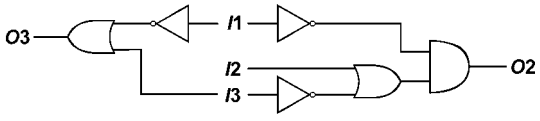

*I*1	*I*2	*I*3	*O*1	*O*2	*O*3
0	*0*	*0*	*0*	*1*	*1*
0	*0*	*1*	*0*	*0*	*1*
0	*1*	*0*	*0*	*1*	*1*
1	*0*	*0*	*0*	*0*	*0*
0	*1*	*1*	*0*	*1*	*1*
1	*0*	*1*	*0*	*0*	*1*
1	*1*	*0*	*0*	*0*	*0*
1	*1*	*1*	*0*	*0*	*1*

Fig. 10. The truth table illustrates the signal transduction behavior of the optical network of Figure 9. The output ***O*1** is always *0* and it is not influenced by the three inputs. Only two inputs determine the value of ***O*3**, while all of them control the output ***O*2**.

(***O*1**, ***O*2**, and ***O*3**) when positive logic conventions are applied to all signals. The equivalent logic circuit shows that all three inputs control the anthracene channel ***O*2**, but only ***I*1** and ***I*3** influence the tetracene channel ***O*3**. Instead, the intensity of the naphthalene channel ***O*1** is always low and it is not affected by the three inputs.

7. Molecule-Based Logic Devices

The signal transduction behavior of the molecular switches in Figures 4 and 6–8 was analyzed exclusively in solution using a combination of conventional spectroscopic techniques.[40–68] These fundamental studies have demonstrated that logic functions can be implemented in chemical systems relying on chemical, electrical, and/or optical signals. These molecular switches, however, remain far from applications in information technology at this stage. The integration of liquid compo-

  0935-9648/02/0603-0410 $ 17.50+.50/0

nents in digital circuits is certainly not practical. Furthermore, most of the logic operations executed rely on bulk addressing. Even although the molecular components of these chemical systems have nanoscaled dimensions, macroscopic collections of them are actually employed for digital processing. In some instances, the operating principles cannot even be scaled down to the unimolecular level, since bulk properties are responsible for signal transduction. Methods to transfer the switching mechanisms developed in solution to miniaturized molecule-based solid-state devices must be developed.

Borrowing designs and fabrication strategies from conventional electronics, the integration of molecular components into real circuits is starting to be explored. A few prototypes have been developed already[69–86] and, in some cases, elementary logic functions could be implemented.[87–92] Generally, these devices are fabricated using a combination of lithography and surface chemistry and, often, consist of pairs of electrodes bridged by nanometer-thick organic films or even single molecules. The behavior of the resulting electrode/organic layer/electrode junctions is dictated by the design of the molecular components. In most instances, electron transfer processes and/or molecular motions govern the interplay between the electrical inputs and outputs of these devices.

The composite assembly illustrated in Figure 11 is a solid-state device incorporating redox active molecules.[77,88] It was fabricated following a stepwise procedure. First, a pattern of parallel electrodes (width = 6 μm) consisting of Al wires covered by a passivating layer of Al_2O_3 was prepared lithographically on a silicon chip. Then, a monolayer of electroactive molecules was deposited on the entire substrate using the Langmuir–Blodgett technique. Finally, an electrode (width = 11 μm) consisting of a bottom Ti wire covered by a thicker Al layer was deposited through a mask by electron-beam evaporation. For clarity, only the portions of the monolayers sandwiched between the top and bottom electrodes are shown in the diagram of Figure 11. The [2]rotaxane **8** is one of the three compounds that were used to assemble this type of devices. The other two molecules were a [3]rotaxane incorporating another crown ether around the second bipyridinium unit and the tetracationic backbone alone. The current/voltage behavior was very similar in the three cases. In fact, all species incorporate bipyridinium units that can be reduced reversibly and phenoxy rings that are oxidized irreversibly. When the potential of one of the bottom electrodes is scanned from 0 to –2 V, a gradual change in current from 0 to 6.5 pA is detected at the top electrode. Approximately the same current response is obtained after resetting the potential to 0 V and scanning it again over the same range. The relatively high current passing through the molecular layer is a result of electron tunneling from the bottom electrode to the bipyridinium centered LUMOs and then from the molecular states to the top electrode. If the potential is scanned from 0 to +2 V and then back to –2 V, no current can be detected at the top electrode. Between +0.7 and +0.9 V, the phenoxy rings of the molecular components are oxidized irreversibly and the "conducting" ability of the molecular layer at negative potentials is lost.

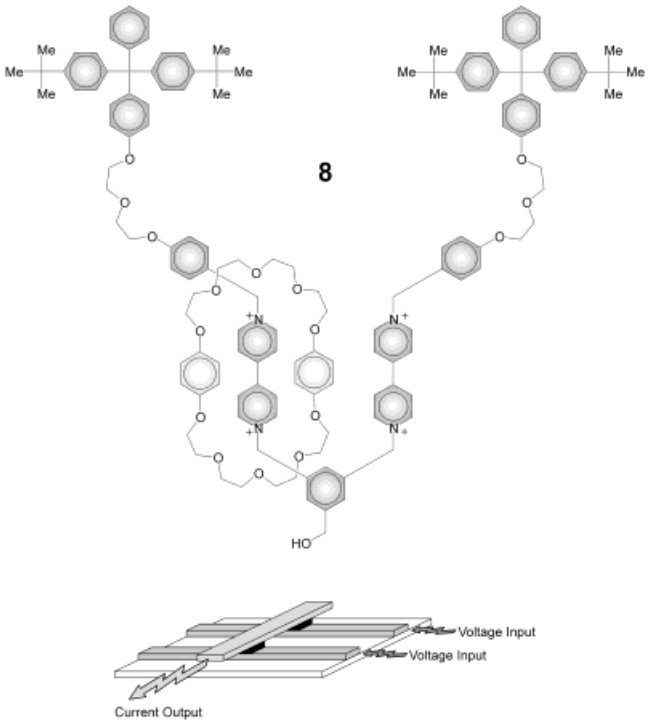

Voltage	Voltage	Current
Low	Low	High
Low	High	Low
High	Low	Low
High	High	Low

Fig. 11. A Ti/Al electrode bridges two parallel Al/Al_2O_3 wires deposited on a silicon chip. The two bottom electrodes are covered by a monolayer of the electroactive [2]rotaxane **8**. For clarity, only the portions of the monolayers sandwiched between the top and bottom electrodes are shown in the diagram. Independent voltage inputs address the two bottom electrodes producing a current output at the top electrode. The current is high only when both voltage inputs are low. If a negative logic convention is applied to both inputs (low = *1*, high = *0*) and a positive logic convention is applied to the output (low = *0*, high = *1*), the signal transduction of operation in this device translates into the truth table of an AND gate.

Simple logic operations could be implemented in the device that incorporates the [2]rotaxane **8** by stimulating the two bottom electrodes with voltage inputs (***I*1** and ***I*2**) and measuring a current output (***O***) at the common top electrode.[88] When at least one of the two inputs is high (0 V), the output is low (< 0.7 nA). When both inputs are low (–2 V), the output is high (ca. 4 nA). If a negative logic convention is applied to the voltage inputs (low = *1*, high = *0*) and a positive logic convention is applied to the current output (low = *0*, high = *1*), the signal transduction behavior translates into the truth table of an AND gate. The output ***O*** is *1* only when both inputs are *1*. If the logarithm of the current is considered as the output, however, an OR operation can be executed. In fact, the logarithm of the current is –12 when both voltage inputs are 0 V. It rises to ca. –9 when one or both voltage inputs are lowered to –2 V. This signal transduction behavior translates into the truth table of an OR gate if, once again, a negative logic convention is applied to the voltage inputs (low = *1*, high = *0*) and

  0935-9648/02/0603-0411 $ 17.50+.50/0

a positive logic convention is applied to the current output (low = *0*, high = *1*). The output ***O*** is *1* when at least one of the two inputs is *1*.

Each electrode/monolayer/electrode junction of the molecule-based device in Figure 11 has a contact area of ca. 66 μm^2 and, therefore, comprises a relatively large number of molecules. The transition from microscaled to nanoscaled junctions can be realized modifying considerably the device architecture.[76] The cross-sectional view in Figure 12a shows a composite assembly in which a monolayer of the thiol **9** is embedded between two gold electrodes mounted on a Si_3N_4 support.[89] This device was fabricated combining chemical vapor deposition, lithography, and anisotropic etching with the self-assembly of the thiols on the surface of the bowl-shaped electrode. In the resulting electrode/monolayer/electrode junction, the contact area is less than 2000 nm^2 and comprises approximately 1000 molecules.

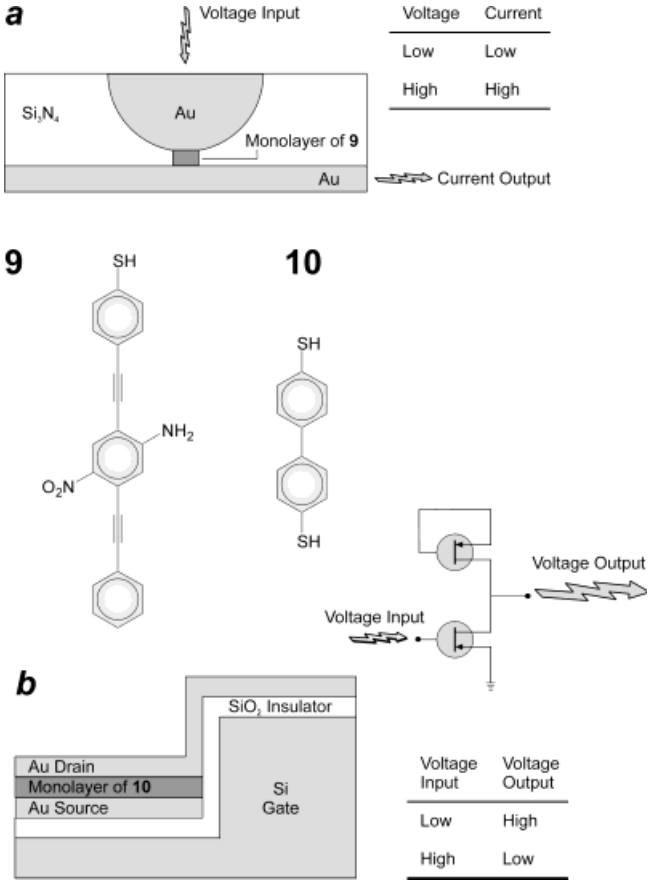

Fig. 12. a) A monolayer of the thiol **9** is embedded between two Au electrodes maintained in position by a Si_3N_4 support. The conductivity of the electrode/monolayer/electrode junction switches from a low to a high value, when a positive (high) voltage pulse is applied to the bowl-shaped electrode. The high-conducting mode is "memorized" by the molecule-based devices and it is retained for more than 15 min. The low-conducting mode can be restored by applying a negative (low) voltage pulse to the same electrode. b) A monolayer of the bisthiol **10** is positioned between two Au electrodes. The current flowing between source and drain can be modulated varying the voltage a Si gate. The molecules within 5 nm from the monolayer/insulator interface determine the current response of the device. An inverter can be assembled pairing two of these molecule-based field-effect transistors. When the voltage input is low, the voltage output is high and vice versa. This signal transduction behavior translates into the truth table of a NOT gate, if a positive logic convention (low = *0*, high = *1*) is applied to the input and output voltages.

The conductivity of the sandwiched monolayer switches reversibly between low and high values, when voltage pulses are applied to one electrode. In the initial state, the monolayer is in a low-conducting mode. A current output of only 30 pA is detected when a probing voltage of +0.25 V is applied to the bowl-shaped electrode. However, the monolayer switches to a high-conducting mode, if the same electrode is stimulated with a short voltage pulse of +5 V. Now, a current output of 150 pA is measured at the same probing voltage of +0.25 V. Repeated probing of the current output at various intervals of time indicates that the high-conducting state is "memorized" by the molecule-based device and it is retained for more than 15 min. The low-conducting mode is restored either after a relatively long period of time or after the stimulation of the bowl-shaped electrode with a reverse voltage pulse of –5 V. In summary, the current output switches from a low to a high value, if a high-voltage input is applied, and from a high to a low value, under the influence of a low-voltage pulse. This behavior offers the unique opportunity of storing and erasing binary data in analogy to a conventional random access memory (RAM).[25] In fact, binary digits can be encoded on the current output of the molecule-based device applying a positive logic convention (low = *0*, high = *1*). It follows that a binary *1* can be stored in the molecule-based device applying a high-voltage input and it can be erased applying a low-voltage input.

The electrode/monolayer/electrode junctions of the composite assemblies in Figure 11 and 12a are two-terminal devices. A voltage input is applied to one terminal and a current output is measured at the other. Transistors, instead, are three-terminal devices. They have a third electrode that gates the current flowing between the source and drain terminals. This type of devices are much more versatile than their two-terminal counterparts for the implementation of logic functions. However, the incorporation of molecular components in a three-terminal configuration is considerably more challenging. A remarkable example is the composite assembly in Figure 12b.[91] This field-effect transistor integrates a monolayer of the bisthiol **10** and three electrodes. Conventional lithography and anisotropic etching were employed to define a vertical step in a doped silicon substrate. The resulting structure was covered with an insulating layer of SiO_2 (thickness = 30 nm) and, then, gold was evaporated on the "bottom" part of the step. On the resulting gold platform, a monolayer of the bisthiol **10** was assembled. Finally, another layer of gold was evaporated on the organic film. Under the influence of the gate voltage, the molecular components embedded in this device modulate the current flowing between the source and drain electrodes. In fact, the intensity of the drain current increases by five orders of magnitude when the gate voltage is lowered below –0.2 V while the source voltage is maintained constant. It is important to note, however, that only the molecules within 5 nm from the monolayer/insulator interface are responsible for conduction. Thus, the current/voltage behavior

0935-9648/02/0603-0412 $ 17.50+.50/0

of this three-terminal device is determined only by a few thousand molecules.

Conventional transistors are the basic building blocks of digital circuits.[26] They are routinely interconnected with specific configurations to execute designed logic functions. The molecule-based transistor in Figure 12b is no exception. It can be used to assemble real electronic circuits incorporating molecular components. This tremendous opportunity was demonstrated experimentally connecting the drain terminals of two molecule-based transistors to afford an inverter.[91] In this basic circuit, an output voltage switches from a high (0 V) to a low value (–2 V) when an input voltage varies from a low (–2 V) to a high value (0 V) and vice versa. This signal transduction behavior translates into the truth table of a NOT gate, if a positive logic convention (low = *0*, high = *1*) is applied to the input and output voltages.

The molecule-based devices in Figure 11 and 12 are closely related to conventional electronics. Their realization demonstrates that organic molecules can be the active components of electronic memory elements, switches, and transistors, and that simple circuits can be assembled with these devices. These outstanding examples are major innovations in molecular electronics and are extremely promising for the realization of nanoscaled devices. At this stage, however, their overall dimensions remain fairly large. The size of their molecular junctions can be certainly reduced to the nanoscale[76] and the conduction through individual molecules can be ensured dispersing the active species in a matrix of inert compounds.[92] However, relatively large device sizes are needed to satisfy these conditions. Methods to miniaturize the actual electrodes, and not only their contact areas, must be developed. On this front, the use of nanocantilevers,[69,72,74,82,85,86] nanoparticles,[80] nanotubes,[93,94] and nanowires[75,79,83,84,95] seems to be extremely promising. If practical strategies to front the obvious challenges in interfacing and connecting these nanocomponents emerge, nanoelectronic circuits combining ultraminiaturized electrodes with unimolecular junctions will appear in the near future.

8. Conclusions

The growing demand for faster computers and internet applications is encouraging the exploration of innovative materials and operating principles for digital processing and communication. A number of elegant strategies to execute logic operations relying on chemical[39–68] and biochemical[96–103] systems have emerged. Chemical, electrical, or optical stimulations can be transduced into specific output signals through controlled transformations of molecular components. Exploiting this operating mechanism, the basic logic operations of AND, NOT, and OR gates have been reproduced relying on simple molecular switches.[39–56] In addition, the molecular design can be adjusted to program certain chemical systems to execute sequences of elementary logic operations.[57–68] Logic functions requiring multiple AND, NOT, and OR gates can be integrated into a single molecular switch or in ensembles of communicating molecules. These beautiful and clever examples of signal processing with chemical systems demonstrate that even simple molecules can speak the complex language of information technology. At the present stage, however, they remain rudimentary examples of digital processors. Practical applications in electronics and photonics might emerge in the future only after considerable fundamental studies on various aspects of this research area. One of the major challenges is the identification of methods to incorporate these functional molecules into solid-state devices while maintaining their signal transduction abilities. The prototypes[69–89] developed so far and the strategies emerged to extrapolate these concepts from isolated molecular switches to chemical networks[66–68] are extremely encouraging. The fabrication of nanoelectronic circuits and all-optical networks from molecular components can be envisaged. Time will tell if these promising functional materials will lead to the development of a new generation of digital devices for information technology.

Received: November 12, 2001
Final version: January 2, 2002

[1] *International Technology Roadmap for Semiconductors*, International SEMATECH, Austin, TX **2000**.
[2] D. Goldhaber-Gordon, M. S. Montemerlo, J. C. Love, G. J. Opiteck, J. C. Ellenbogen, *Proc. IEEE* **1997**, *85*, 521.
[3] D. A. Muller, T. Sorsch, S. Moccio, F. H. Baumann, K. Evans-Lutterodt, G. Timp, *Nature* **1999**, *399*, 758.
[4] J. D. Meindl, Q. Chen, J. D. Davies, *Science* **2001**, *293*, 2044.
[5] M. Schultz, *Nature* **1999**, *399*, 729.
[6] Special issue on "Optical networking": *Bell Labs Tech. J.* **1999**, *4(1)*, 3.
[7] A. M. Glass, D. J. Di Giovanni, T. A. Strasser, A. J. Stentz, R. E. Slusher, A. E. White, A. R. Kortan, B. J. Eggleton, *Bell Labs Tech. J.* **2000**, *5(1)*, 168.
[8] J. M. Kahn, K.-P. Ho, *Nature* **2001**, *411*, 1007.
[9] P. P. Mitra, J. B. Stark, *Nature* **2001**, *411*, 1027.
[10] L. Thylen, G. Karlsson, O. Nilsson, *IEEE Commun. Mag.* **1996**, *34(2)*, 106.
[11] N. A. Jackman, S. H. Patel, B. P. Mikkelsen, S. K. Korotky, *Bell Labs Tech. J.* **1999**, *4(1)*, 262.
[12] M. Veeraraghavan, R. Karri, T. Moors, M. Karol, R. Grobler, *IEEE Commun. Mag.* **2001**, *39(3)*, 118.
[13] A. J. Bard, *Integrated Chemical Systems: a Chemical Approach to Nanotechnology*, Wiley, New York **1994**.
[14] A. P. Alivisatos, P. F. Barbara, A. W. Castleman, J. Chang, D. A. Dixon, M. L. Klein, G. L. McLendon, J. S. Miller, M. A. Ratner, P. J. Rossky, S. I. Stupp, M. E. Thompson, *Adv. Mater.* **1998**, *10*, 1297.
[15] Special issue on "Photochromism: memories and switches", *Chem. Rev.* **2000**, *100*, 1683–1890.
[16] Special issue on "Molecular machines", *Acc. Chem. Res.* **2001**, *34*, 409–522.
[17] L. M. Tolbert, *Acc. Chem. Res.* **1992**, *25*, 561.
[18] S. Yitzchaik, T. J. Marks, *Acc. Chem. Res.* **1996**, *29*, 197.
[19] C. Y. Liu, A. J. Bard, *Acc. Chem. Res.* **1999**, *32*, 235.
[20] R. M. Metzger, *Acc. Chem. Res.* **1999**, *32*, 950.
[21] J. M. Tour, *Acc. Chem. Res.* **2000**, *33*, 791.
[22] C. Joachim, J. K. Gimzewski, A. Aviram, *Nature* **2000**, *408*, 541.
[23] A. N. Shipway, I. Willner, *Acc. Chem. Res.* **2001**, *34*, 421.
[24] A. R. Pease, J. O. Jeppesen, J. F. Stoddart, Y. Luo, C. P. Collier, J. R. Heath, *Acc. Chem. Res.* **2001**, *34*, 433.
[25] R. J. Mitchell, *Microprocessor Systems: An Introduction*, Macmillan, London **1995**.
[26] S. Madhu, *Electronics: Circuits and Systems*, SAMS, Indianapolis **1985**.
[27] M. A. Karim, A. A. S. Awwal, *Optical Computing: An Introduction*, Wiley, New York **1992**.
[28] *Molecular Switches* (Ed: B. L. Feringa), Wiley-VCH, Weinheim **2001**.
[29] L. Fabbrizzi, M. Licchelli, P. Pallavicini, *Acc. Chem. Res.* **1999**, *32*, 846.
[30] I. Willner, E. Katz, *Angew. Chem. Int. Ed.* **2000**, *39*, 1180.

  0935-9648/02/0603-0413 $ 17.50+.50/0

[31] V. Balzani, A. Credi, F. M. Raymo, J. F. Stoddart, *Angew. Chem. Int. Ed.* **2000**, *39*, 3348.
[32] M. Irie, *Chem. Rev.* **2000**, *100*, 1685.
[33] Y. Yokoyama, *Chem. Rev.* **2000**, *100*, 1717.
[34] G. Berkovic, V. Krongauz, V. Weiss, *Chem. Rev.* **2000**, *100*, 1741.
[35] B. L. Feringa, R. A. van Delden, N. Koumura, E. M. Geertsema, *Chem. Rev.* **2000**, *100*, 1789.
[36] B. L. Feringa, *Acc. Chem. Soc.* **2001**, *101*, 504.
[37] F. Diederich, *Chem. Commun.* **2001**, 219.
[38] D. Kuciauskas, P. A. Liddell, A. L. Moore, T. A. Moore, D. Gust, *J. Am. Chem. Soc.* **1998**, *120*, 10 880.
[39] A. Aviram, *J. Am. Chem. Soc.* **1988**, *110*, 5687.
[40] A. P. de Silva, H. Q. N. Gunaratne, C. P. McCoy, *Nature* **1993**, *364*, 42.
[41] A. P. de Silva, A. A. de Silva, A. S. Dissanayake, K. R. A. S. Sandanayake, *J. Chem. Soc., Chem. Commun.* **1989**, 1054.
[42] A. P. de Silva, S. A. de Silva, *J. Chem. Soc., Chem. Commun.* **1986**, 1709.
[43] A. P. de Silva, K. R. A. S. Sandanayake, *J. Chem. Soc., Chem. Commun.* **1989**, 1183.
[44] A. P. de Silva, H. Q. N. Gunaratne, G. E. M. Maguire, *J. Chem. Soc., Chem. Commun.* **1994**, 1213.
[45] I. Iwata, K. Tanaka, *J. Chem. Soc., Chem. Commun.* **1995**, 1491.
[46] C. R. Cooper, T. D. James, *Chem. Commun.* **1997**, 1419.
[47] P. Ghosh, P. K. Bharadwaj, S. Mandal, S. Ghosh, *J. Am. Chem. Soc.* **1996**, *118*, 1553.
[48] A. P. de Silva, H. Q. N. Gunaratne, C. P. McCoy, *J. Am. Chem. Soc.* **1997**, *119*, 7891.
[49] P. Ghosh, P K. Bharadwaj, J. Roy, S. Ghosh, *J. Am. Chem. Soc.* **1997**, *119*, 11 903.
[50] M. Inouye, K. Akamatsu, H. Nakazumi, *J. Am. Chem. Soc.* **1997**, *119*, 9160.
[51] F. Pina, A. Roque, M. J. Melo, I. Maestri, L. Belladelli, V. Balzani, *Chem. Eur. J.* **1998**, *4*, 1184.
[52] L. Gobbi, P. Seiler, F. Diederich, *Angew. Chem. Int. Ed.* **1999**, *38*, 674.
[53] L. Gobbi, P. Seiler, F. Diederich, V. Gramlich, C. Boudon, J. P. Gisselbrecht, M. Gross, *Helv. Chim. Acta* **2001**, *84*, 743.
[54] A. S. Lukas, P. J. Bushard, M. R. Wasielewski, *J. Am. Chem. Soc.* **2001**, *123*, 2440.
[55] R. Herges, M. Deichmann, J. Grunenberg, G. Bucher, *Chem. Phys. Lett.* **2000**, *327*, 149.
[56] K. L. Kompa, R. D. Levine, *Proc. Natl. Acad. Sci. USA* **2001**, *98*, 410.
[57] T. Gunnlaugsson, D. A. Mac Donail, D. Parker, *Chem. Commun.* **2000**, 93.
[58] A. P. de Silva, I. M. Dixon, H. Q. N. Gunaratne, T. Gunnlaugsson, P. R. S. Maxwell, T. E. Rice, *J. Am. Chem. Soc.* **1999**, *121*, 1393.
[59] A. Roque, F. Pina, S. Alves, R. Ballardini, M. Maestri, V. Balzani, *J. Mater. Chem.* **1999**, *9*, 2265.
[60] A. Credi, V. Balzani, S. J. Langford, J. F. Stoddart, *J. Am. Chem. Soc.* **1997**, *119*, 2679.
[61] F. Pina, M. J. Melo, M. Maestri, P. Passaniti, V. Balzani, *J. Am. Chem. Soc.* **2000**, *122*, 4496.
[62] M. Asakawa, P. R. Ashton, V. Balzani, A. Credi, G. Mattersteig, O. A. Matthews, M. Montalti, N. Spencer, J. F. Stoddart, M. Venturi, *Chem. Eur. J.* **1997**, *3*, 1992.
[63] A. P. de Silva, N. D. McClenaghan, *J. Am. Chem. Soc.* **2000**, *122*, 3965.
[64] H. F. Ji, R. Dabestani, G. M. Brown, *J. Am. Chem. Soc.* **2000**, *122*, 9306.
[65] F. M. Raymo, S. Giordani, *J. Am. Chem. Soc.* **2001**, *123*, 4651.
[66] F. M. Raymo, S. Giordani, *Org. Lett.* **2001**, *3*, 1833.
[67] F. M. Raymo, S. Giordani, *Org. Lett.* **2001**, *3*, 3475.
[68] F. M. Raymo, S. Giordani, *J. Am. Chem. Soc.* **2002**, *124*, in press.
[69] M. Pomerantz, A. Aviram, R. A. McCorkle, L. Li, A. G. Schrott, *Science* **1992**, *255*, 1115.
[70] A. S. Martin, J. R. Sambles, G. J. Ashwell, *Phys. Rev. Lett.* **1993**, *70*, 218.
[71] C. M. Fischer, M. Burghard, S. Roth, K. v. Klitzing, *Appl. Phys. Lett.* **1995**, *66*, 3331.
[72] L. A. Bumm, J. J. Arnold, M. T. Cygan, T. D. Dunbar, T. P. Burgin, L. Jones II, D. L. Allara, J. M. Tour, *Science* **1996**, *271*, 1705.
[73] R. M. Metzger, B. Chen, U. Hopfner, M. V. Lakshmikantham, D. Vuillaume, T. Kawai, X. Wu, H. Tachibana, T. V. Hughes, H. Sakurai, J. W. Baldwin, C. Hosch, M. P. Cava, L. Brehmer, G. J. Ashwell, *J. Am. Chem. Soc.* **1997**, *119*, 10 455.
[74] C. Joachim, J. K. Gimzewski, H. Tang, *Phys. Rev. B* **1998**, *58*, 16 407.
[75] M. A. Reed, C. Zhou, C. J. Muller, T. P. Burgin, J. M. Tour, *Science* **1997**, *278*, 252.
[76] J. Chen, M. A. Reed, A. M. Rawlett, J. M. Tour, *Science* **1999**, *286*, 1550.
[77] E. W. Wong, C. P. Collier, M. Belohradsky, F. M. Raymo, J. F. Stoddart, J. R. Heath, *J. Am. Chem. Soc.* **2000**, *122*, 5831.
[78] K. M. Roth, N. Dontha, R. B. Dabke, D. T. Gryko, C. Clausen, J. S. Lindsey, D. F. Bocian, W. G. Kuhr, *J. Vac. Sci. Tech. B* **2000**, *18*, 2359.
[79] H. Park, J. Park, A. K. L. Lim, E. H. Anderson, A. P. Alivisatos, P. L. McEuen, *Nature* **2000**, *407*, 57.
[80] D. I. Gittins, D. Bethell, D. J. Schiffrin, R. J. Nichols, *Nature* **2000**, *408*, 67.
[81] C. P. Collier, G. Mattersteig, E. W. Wong, Y. Luo, K. Beverly, J. Sampaio, F. M. Raymo, J. F. Stoddart, J. R. Heath, *Science* **2000**, *289*, 1172.
[82] F.-R. F. Fan, J. Yang, S. M. Dirk, D. W. Price, D. Kosynkin, J. M. Tour, A. J. Bard, *J. Am. Chem. Soc.* **2001**, *123*, 2454.
[83] A. Bogozi, O. Lam, H. X. He, C. Z. Li, N. J. Tao, L. A. Nagahara, I. Amlani, R. Tsui, *J. Am. Chem. Soc.* **2001**, *123*, 4585.
[84] H. X. He, J. S. Zhu, N. J. Tao, L. A. Nagahara, I. Amlani, R. Tsui, *J. Am. Chem. Soc.* **2001**, *123*, 7730.
[85] Z. J. Donhauser, B. A. Mantooth, K. F. Kelly, L. A. Bumm, J. D. Monnell, J. J. Stapleton, D. W. Price, A. M. Rawlett, D. L. Allara, J. M. Tour, P. S. Weiss, *Science* **2001**, *292*, 2303.
[86] X. D. Cui, A. Primak, X. Zarate, J. Tomfohr, O. F. Sankey, A. L. Moore, T. A. Moore, D. Gust, G. Harris, S. M. Lindsay, *Science* **2001**, *294*, 571.
[87] F. Patolsky, B. Filanovsky, E. Katz, I. Willner, *J. Phys. Chem. B* **1998**, *102*, 10 359.
[88] C. P. Collier, E. W. Wong, M. Belohradsky, F. M. Raymo, J. F. Stoddart, P. J. Kuekes, R. S. Williams, J. R. Heath, *Science* **1999**, *285*, 391.
[89] M. A. Reed, J. Chen, A. M. Rawlett, D. W. Price, J. M. Tour, *Appl. Phys. Lett.* **2001**, *78*, 3735.
[90] S. Ami, C. Joachim, *Nanotechnology* **2001**, *12*, 44.
[91] J. H. Schön, H. Meng, Z. Bao, *Nature* **2001**, *413*, 713.
[92] J. H. Schön, H. Meng, Z. Bao, *Science* **2001**, *294*, 2138.
[93] A. Bachtold, P. Hadley, T. Nakanishi, C. Dekker, *Science* **2001**, *294*, 1317.
[94] V. Derycke, R. Martel, J. Appenzeller, P. Avouris, *Nano Lett.* **2001**, *1*, 453.
[95] Y. Huang, X. Duan, Y. Cui, L. J. Lauhon, K.-H. Kim, C. M. Lieber, *Science* **2001**, *294*, 1313.
[96] N. Lotan, G. Ashkenazi, G. Tuchman, S. Nehamkin, S. Sideman, *Mol. Cryst. Liq. Cryst.* **1993**, *236*, 95.
[97] L. M. Adelman, *Science* **1994**, *266*, 1021.
[98] R. R. Birge, *Sci. Am.* **1995**, *272(3)*, 90.
[99] D. Bray, *Nature* **1995**, *376*, 307.
[100] G. Ashkenazi, D. R. Ripoll, N. Lotan, H. A. Scheraga, *Biosens. Bioelectron.* **1997**, *12*, 85.
[101] S. Sivan, N. Lotan, *Biotechnol. Progr.* **1999**, *15*, 964.
[102] E. W. Schlag, S.-Y. Sheu, D. Y. Yang, H. L. Selzle, S. H. Lin, *Proc. Acad. Natl. Sci. USA* **2000**, *97*, 1068.
[103] F. Xu, E. J. Golightly, K. R. Duke, S. F. Lassen, B. Knusen, S. Christenses, K. M. Brown, S. H. Brown, M. Schülein, *Enzyme Microb. Tech.* **2001**, *28*, 744.

  0935-9648/02/0603-0414 $ 17.50+.50/0